Supplementary Figures for

BAF complex maintains glioma stem cells in pediatric H3K27M-glioma

Eshini Panditharatna[1,2*], Joana G. Marques[1,2*], Tingjian Wang[3], Maria C. Trissal[1,2], Ilon Liu[1,2], Li Jiang[1,2], Alexander Beck[4], Andrew Groves[1,2], Neekesh V. Dharia[1,2], Deyao Li[3], Samantha E. Hoffman[1,2], Guillaume Kugener[2], McKenzie L. Shaw[1], Hafsa M. Mire[1,2], Olivia A. Hack[1], Joshua M. Dempster[2], Caleb Lareau[2,5], Lingling Dai[3], Logan H. Sigua[3], Michael A. Quezada[6], Ann-Catherine J. Stanton[7], Meghan Wyatt[2], Zohra Kalani[2], Amy Goodale[2], Francisca Vazquez[2], Federica Piccioni[2,8], John G. Doench[2], David E. Root[2], Jamie N. Anastas[9,10], Kristen L. Jones[11], Amy Saur Conway[1], Sylwia Stopka[12], Michael S. Regan[12], Yu Liang[3], Hyuk-Soo Seo[3,13], Kijun Song[3], Puspalata Bashyal[3], William P. Jerome[1], Nathan D. Mathewson[14], Sirano Dhe-Paganon[3,13], Mario L. Suvà[15,16], Angel M. Carcaboso[17], Cinzia Lavarino[17], Jaume Mora[17], Quang-De Nguyen[11], Keith L. Ligon[1,2,18], Yang Shi[9,19], Sameer Agnihotri[7], Nathalie Y. R. Agar[3,12], Kimberly Stegmaier[1,2], Charles D. Stiles[3], Michelle Monje[20], Todd R. Golub[1,2], Jun Qi[3#], Mariella G. Filbin[1,2#]

*Co-first authors.

#Co-corresponding authors:

Mariella G. Filbin

mariella.filbin@childrens.harvard.edu

Jun Qi

Jun_Qi@DFCI.HARVARD.EDU

This PDF file includes:

Supplementary Figures 1 -6

Supplementary Figure 1.

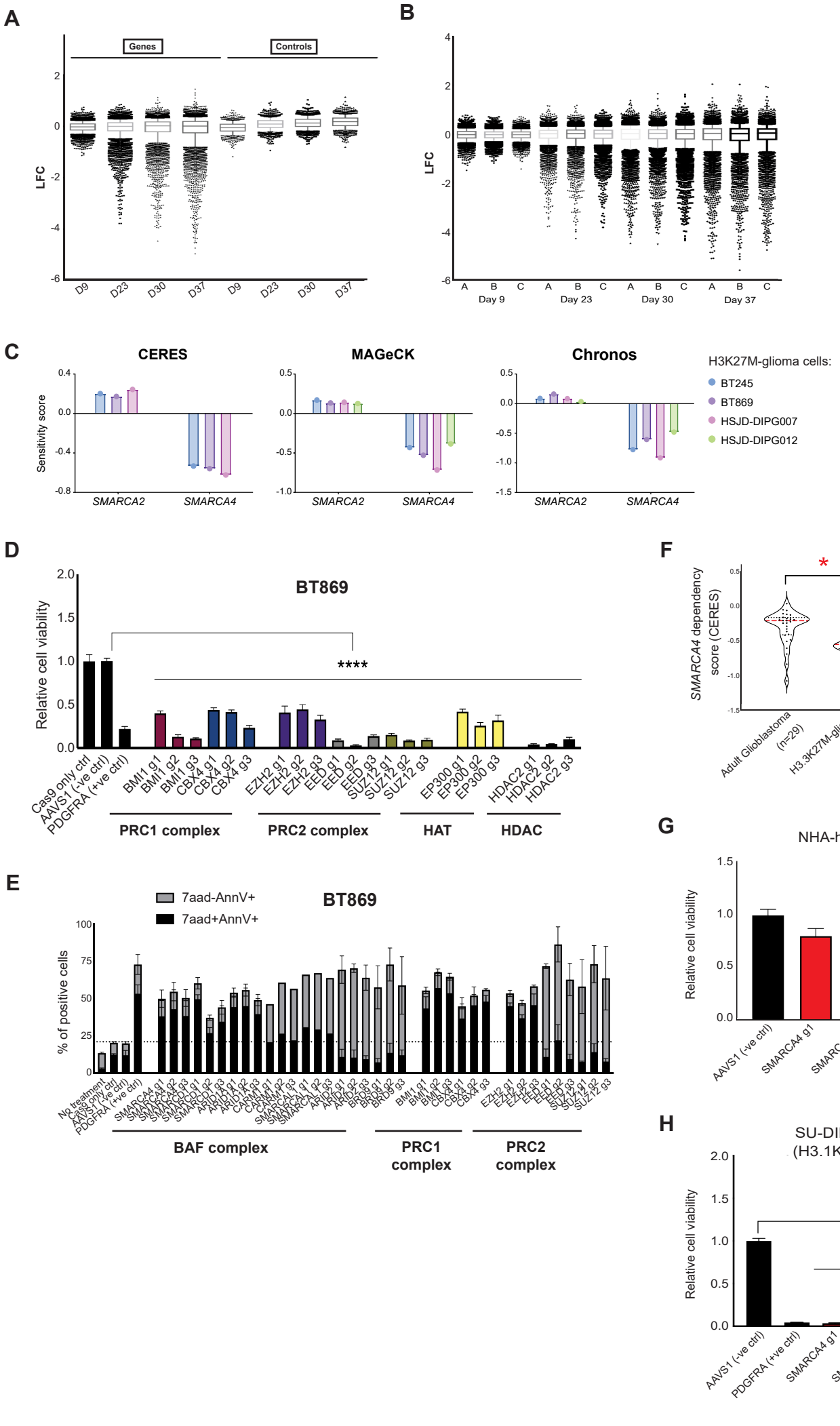

Supplementary figure 1. A. Log fold change (LFC) of dropout rates of single guide RNAs (sgRNAs) targeting 1,350 genes (Genes) and 1,000 non-targeting control sgRNAs (Controls) at days 9, 23, 30, and 37 post infection in epigenetic focused CRISPR/Cas9 screen in four H3.3K27M-glioma neurosphere models. Dependency scores (using MAGeCK, CERES, Chronos algorithms) were subsequently calculated (Table S1-3). **B.** Log fold change (LFC) of dropout rates of sgRNAs targeting 1,350 genes in three replicates (A, B, C) for each timepoint (days 9, 23, 30, and 37 post infection) in epigenetic focused CRISPR/Cas9 screen in four H3.3K27M-glioma neurosphere models. **C.** Sensitivity scores (CERES, MAGeCK, and Chronos) of *SMARCA2* and *SMARCA4* knockouts in four H3K27M-glioma cell lines. Data collected at days 30 and 37 of the CRISPR screen were used to calculate these scores**. D.** Relative cell viability in BT869 (H3.3K27M-glioma) neurosphere model following single gene CRISPR/ Cas9 mediated knockout of PRC1, PRC2 complex, *EP300* and *HDAC2* genes using three different sgRNAs (g1, g2, g3) per gene (normalized to *AAVS1* negative sgRNA control). Data are shown as mean +/- SEM, ****p-value < 0.0001. **E.** Percentage of cells positive for apoptosis (7aad-AnnV+, gray bars) and necrosis (7aad+AnnV+, black bars) analyzed by flow cytometry, upon single gene CRISPR/Cas9 mediated knockout of BAF, PRC1, and PRC2 complex members using three different sgRNAs per gene in BT869 neurospheres. No treatment, Cas9 only, and *AAVS1* sgRNA were used as negative controls, while *PDGFRA* knockout was used as a positive control. **F.** Dependency scores (CERES) for *SMARCA4* in four H3.3K27M-glioma models compared to 29 adult glioblastoma models reported in the Cancer Dependency Map (Broad Institute). **G.** Relative cell viability (normalized to *AAVS1* negative sgRNA control) upon single gene CRISPR/Cas9 mediated knockout of *SMARCA4* using three different sgRNAs (g1, g2, g3) in immortalized normal human astrocytes (NHA-hTERT). AAVS1 negative sgRNA was used as a negative control. Data are shown as mean +/- SEM. **H.** Relative cell viability (normalized to *AAVS1* negative sgRNA control) in SU-DIPGIV (H3.1K27M-glioma) neurosphere model following single gene CRISPR/Cas9 mediated knockout of *SMARCA4* using three different sgRNAs (g1, g2, g3). *AAVS1* negative sgRNA was used as a negative control, while *PDGFRA* knockout was used as a positive control. Data are shown as mean +/- SEM, ****p-value < 0.0001.

Supplementary Figure 2.

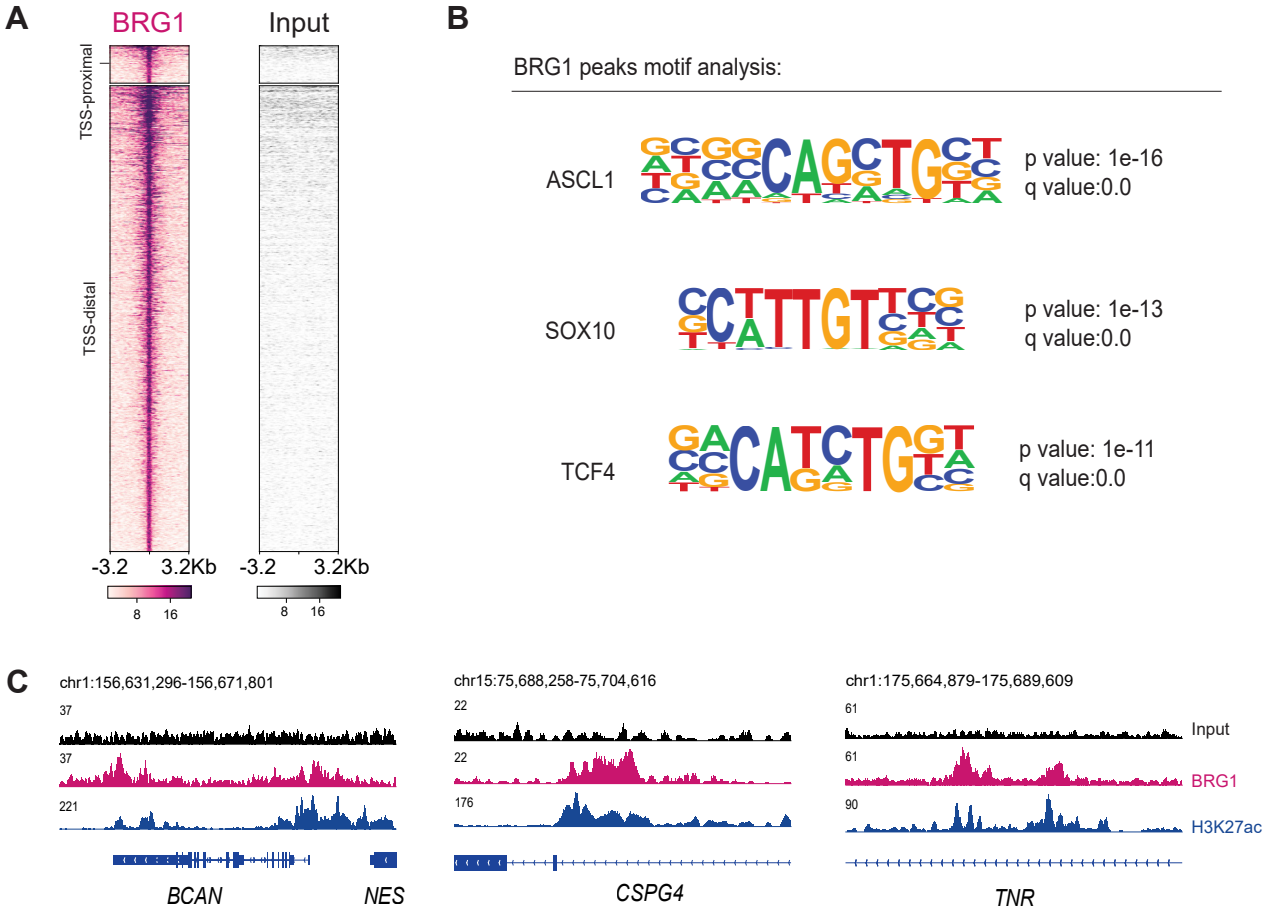

Supplementary figure 2. A. Heatmaps depicting BRG1 ChIPseq and input signal in BT869 (H3.3K27M-glioma) neurospheres at BRG1 binding sites according to their distance to transcription start sites (TSS). Regions within 1kb of the TSS were considered TSS-proximal sites (top, n=99) while all others were classified as TSS-distal (bottom, n=1,236). Each row shows 6.4kb regions, centered on BRG1 peaks and ranked by BRG1 ChIPseq signal intensity. Color shading corresponds to ChIPseq read counts. **B.** Transcription factor motifs enriched in BRG1 binding sites (n=1,335) in BT869 neurospheres as determined by Homer analysis. **C.** Gene tracks display input, BRG1, and H3K27ac ChIPseq signal at promoters and enhancers of OPC-like cancer cell state marker genes (*BCAN*, *CSPG4* and *TNR*).

Supplementary Figure 3.

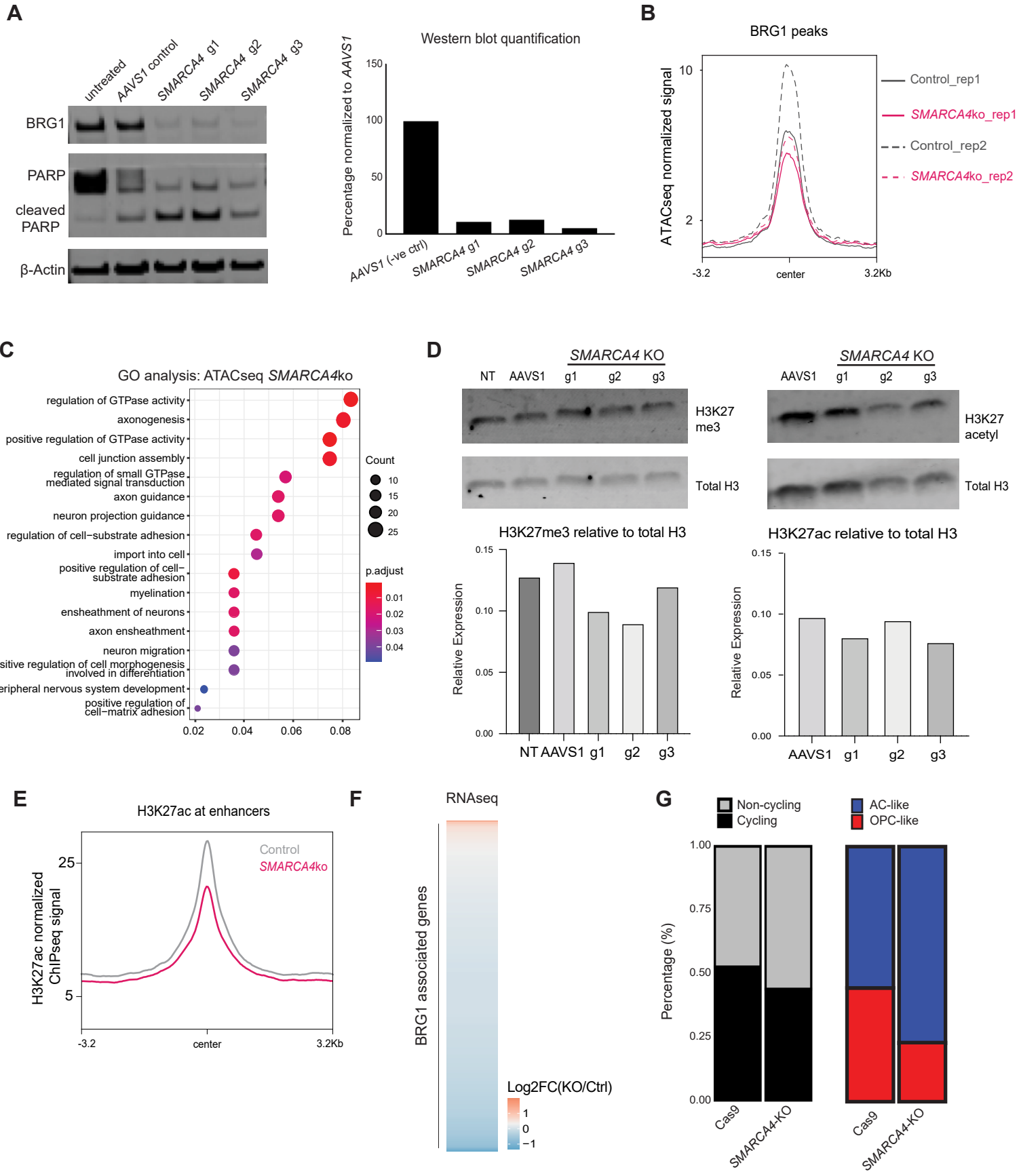

Supplementary figure 3. A. Western blot (left panel) and quantification (right panel) for BRG1, PARP, and cleaved PARP protein levels in BT869 neurospheres four days after *SMARCA4* knockout using three different sgRNAs (g1, g2, g3), compared to *AAVS1* negative sgRNA control. Cleaved PARP was used as a marker for apoptosis, and β-actin was used as a loading control. **B.** Profile plot depicting average ATACseq signal at BRG1 binding sites (n=1,335) in BT869 neurospheres expressing either a guide RNA targeting the *AAVS1* locus (control cells in gray) or *SMARCA4* (pink). ATACseq was conducted four days after nucleofections. The plot shows two replicates (rep), 6.4kb regions, centered on BRG1 peaks. **C.** Biological processes (gene ontology) as determined from regions with decreased ATACseq signal in BT869 neurospheres four days after *SMARCA4* knockout. The number of genes is indicated by the size of the circle, and significance is depicted by the color scale. **D.** Western blots (top panels) depicting H3K27me3 and H3K27ac levels and corresponding quantifications (bottom panels) of histone enriched protein extracts from *SMARCA4* knockout BT869 neurospheres four days after nucleofections, compared to negative controls (*AAVS1* negative sgRNA or NT= no nucleofection control). Left panel shows H3K27 trimethylation and total H3 as loading control. Right panel shows H3K27 acetylation and total H3 as loading control. Bar graphs represent relative quantification compared to total H3. **E.** Profile plot depicting the average H3K27ac ChIPseq signal at all enhancer sites (n=11,492), obtained using the program ROSE, identified in BT869 neurospheres. The plot shows 6.4kb regions, centered on H3K27ac peaks. **F.** Heatmap depicting changes in expression (as $\log_2$) of all genes associated with BRG1 ChIPseq binding sites (n=703) after *SMARCA4* knockout as determined by bulk RNAseq. **G.** Changes in the percentage of cycling vs. non-cycling (left panel), and OPC- vs AC-like cancer cell subpopulations (right panel) in *SMARCA4* knockout and Cas9 control cells four days after knockout in BT869 neurospheres, as determined by scRNAseq analysis.

Supplementary Figure 4.

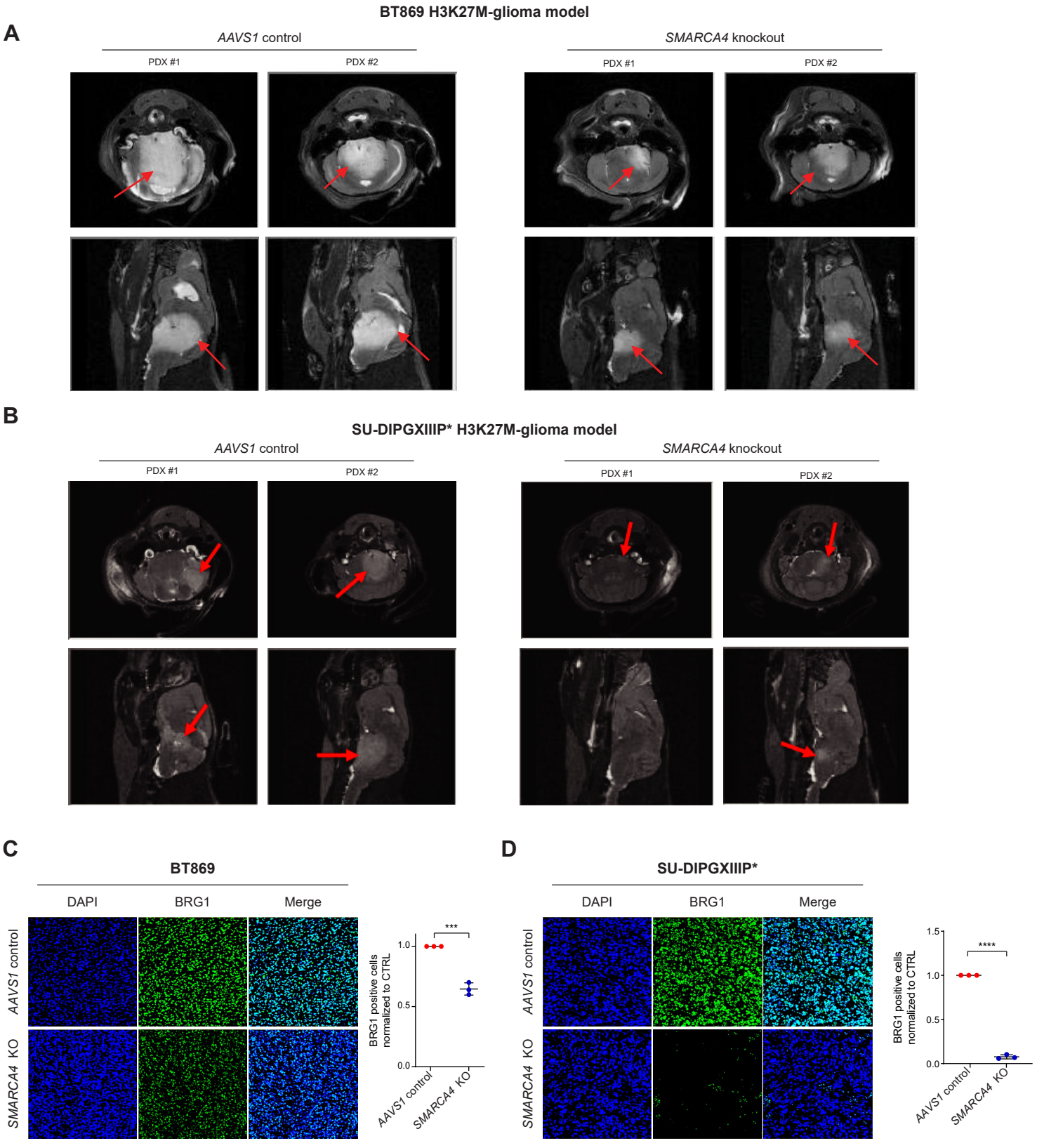

Supplementary figure 4. A. Representative MRIs showing tumors (red arrows) in mice harboring either *AAVS1* negative sgRNA control or *SMARCA4* knockout BT869 (biopsy-derived H3.3K27M model) tumor cells. Top panels show a coronal view and bottom panels show a sagittal view. **B.** Representative MRIs showing tumors (red arrows) in mice bearing either *AAVS1* negative sgRNA control or *SMARCA4* knockout SU-DIPGXIIIP* (autopsy-derived H3.3K27M pontine model) tumor cells. Top panels show a coronal view and bottom panels show a sagittal view. **C.** Representative immunofluorescence images depicting the levels of BRG1 in *AAVS1* control and *SMARCA4* knockout (KO) BT869 PDX tumors collected at end stage disease (left) and respective quantification (right). Data is shown as mean+/-SD (n=3; p-value = 0.0003, unpaired t test). **D.** Representative immunofluorescence images depicting the levels of BRG1 in *AAVS1* control and *SMARCA4* knockout (KO) SU-DIPGXIIIP* PDX tumors collected at the end stage disease (left) and respective quantification (right). Data is shown as mean+/-SD (n=3; p-value <0.0001, unpaired t test).

Supplementary Figure 5.

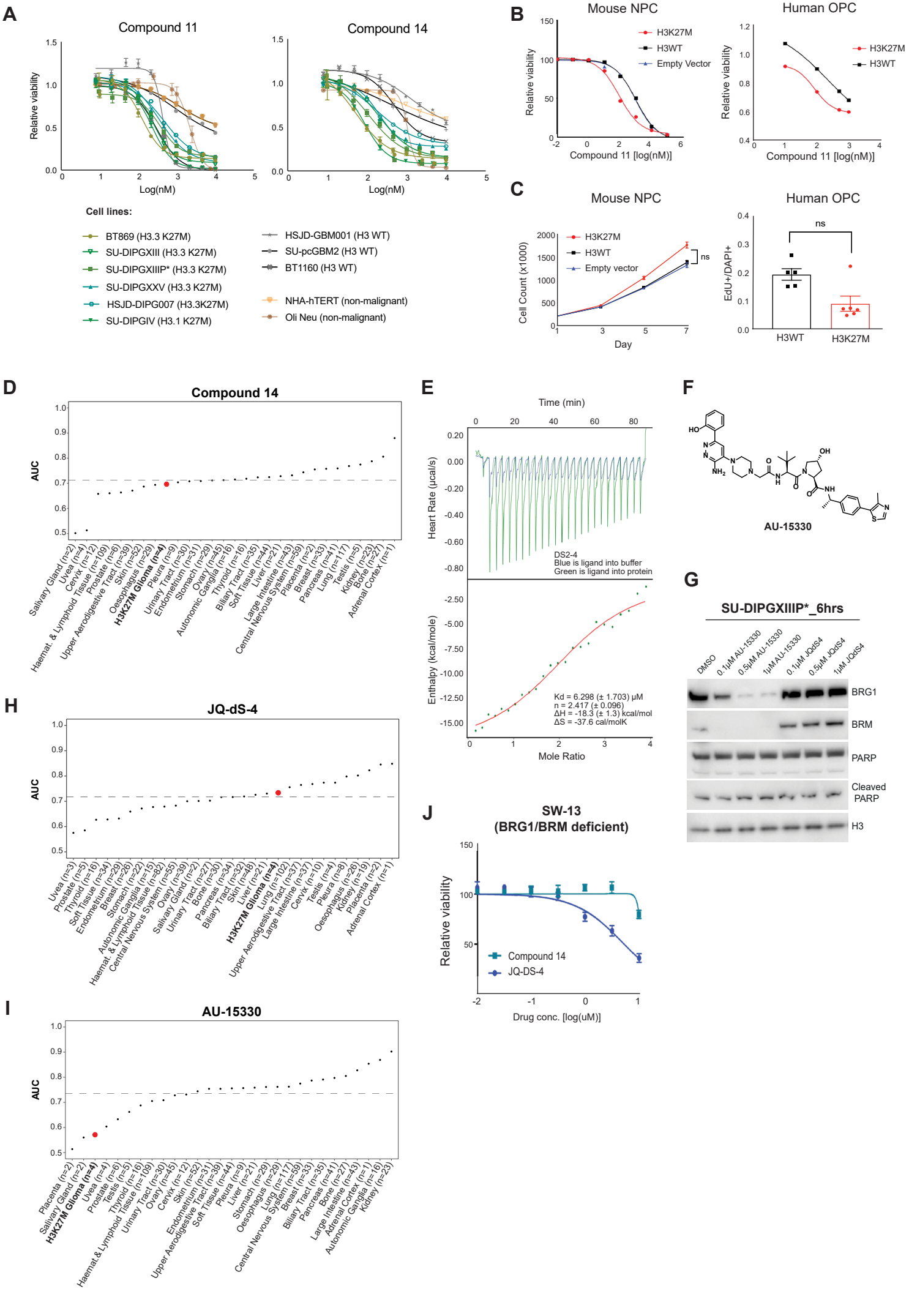

Supplementary figure 5. A. Dose response curves for BRG1/BRM inhibitors (Compounds 11 and 14) in H3.3K27M (n=5), H3.1K27M (n=1), and H3WT (n=3) pediatric glioma neurosphere models, and non-malignant cell lines (n=2, NHA-hTERT: immortalized normal human astrocytes, and Oli Neu: immortalized normal mouse OPCs). **B.** Dose response curves for Compound 11 in mouse NPCs and human OPCs expressing H3K27M, compared to syngeneic control cells expressing H3WT or empty vector. **C.** Relative cell proliferation of mouse NPCs and human OPCs expressing H3K27M compared to syngeneic control cells expressing H3WT or empty vector. **D.** Profiling relative inhibition simultaneously in mixtures (PRISM) analysis of 880 cancer cell lines representing 29 lineages (Broad Institute), treated with Compound 14 at an 8-point dose curve (3-fold dilution, with a maximum of 10 μM) for 5-days. The black dashed line represents the mean AUC computed over cell lines of all lineages. Cancer lineages below this black dashed line represent those sensitive to BRG1/BRM inhibition by Compound 14. **E.** Isothermal calorimetry (ITC) confirms binding of JQ-dS-4 to BRG1 (*SMARCA4*) with a Kd of 6.3 μM. **F.** Chemical structure of BRG1/BRM degrader AU-15330. **G.** Immunoblot for BRG1 and BRM protein levels in SU-DIPGXIIIP* H3.3K27M-glioma neurospheres treated with AU-15330 and JQ-dS-4 at indicated doses for 6 hours. Cleaved PARP levels are shown as a marker for apoptosis. Total H3 served as a loading control. **H.** PRISM analysis of 694 cancer cell lines representing 23 lineages (Broad Institute), treated with JQ-dS-4. The black dashed line represents the mean AUC computed over cell lines of all lineages. Cancer lineages below this black dashed line represent those sensitive to BRG1/BRM degradation by JQ-dS-4. **I.** PRISM analysis of 880 cancer cell lines representing 29 lineages (Broad Institute), treated with AU-15330. The black dashed line represents the mean AUC computed over cell lines of all lineages. Cancer lineages below this black dashed line represent those sensitive to BRG1/BRM degradation by AU-15330. **J.** Dose response curves for Compound 11 and JQ-dS-4 in an adrenocortical carcinoma cell line deficient for BRG1/BRM (SW-13).

Supplementary Figure 6.

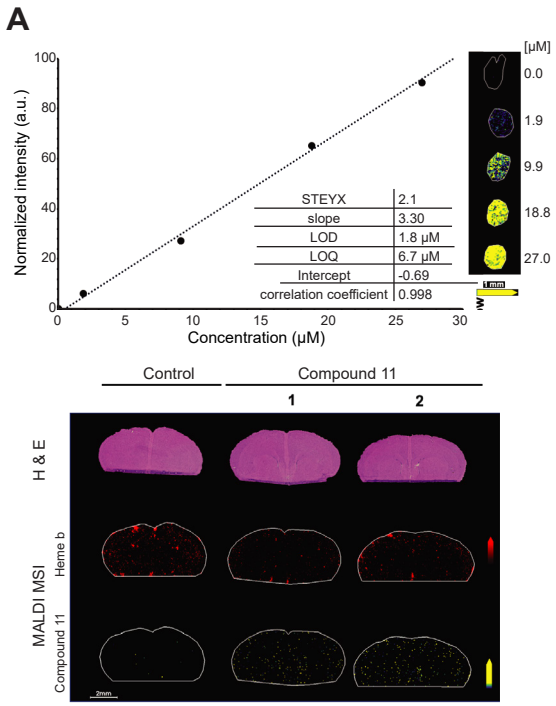

B

Compound	Brain/plasma ratio
Compound 11	0.96%
Compound 12	1.17%
Compound 14	1.04%
JQ-dS-4	2.50%

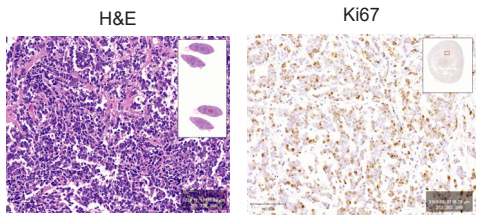

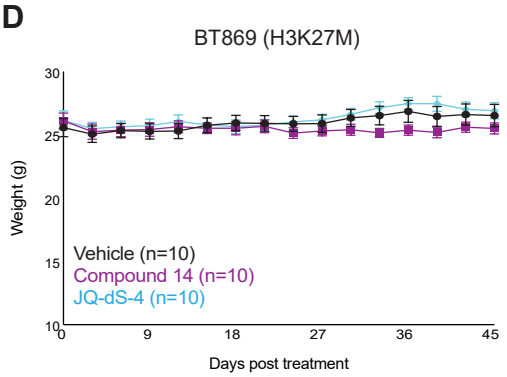

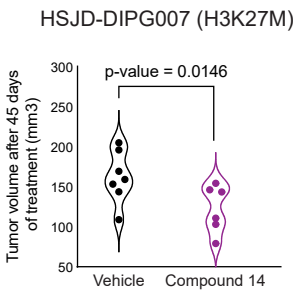

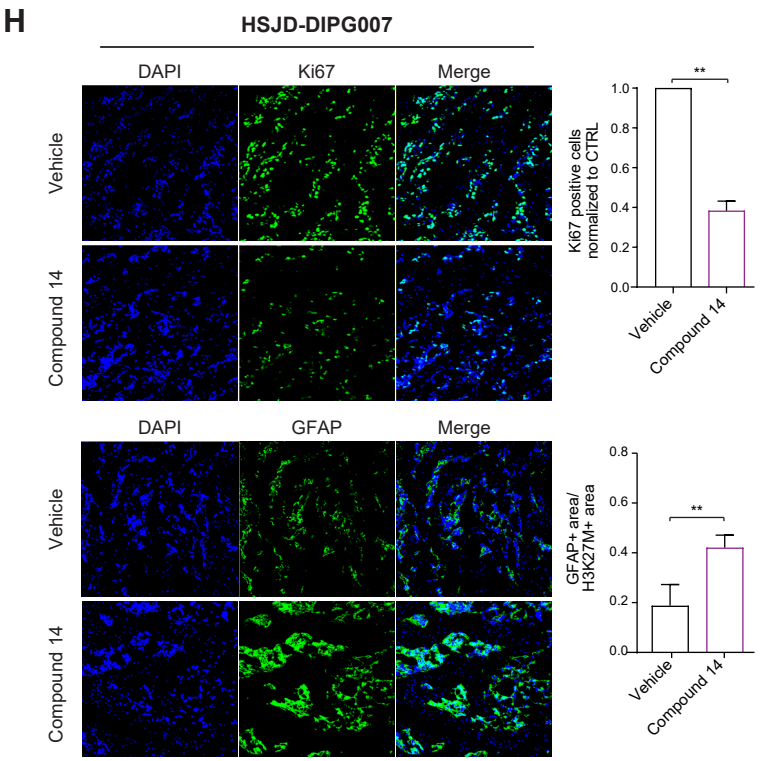

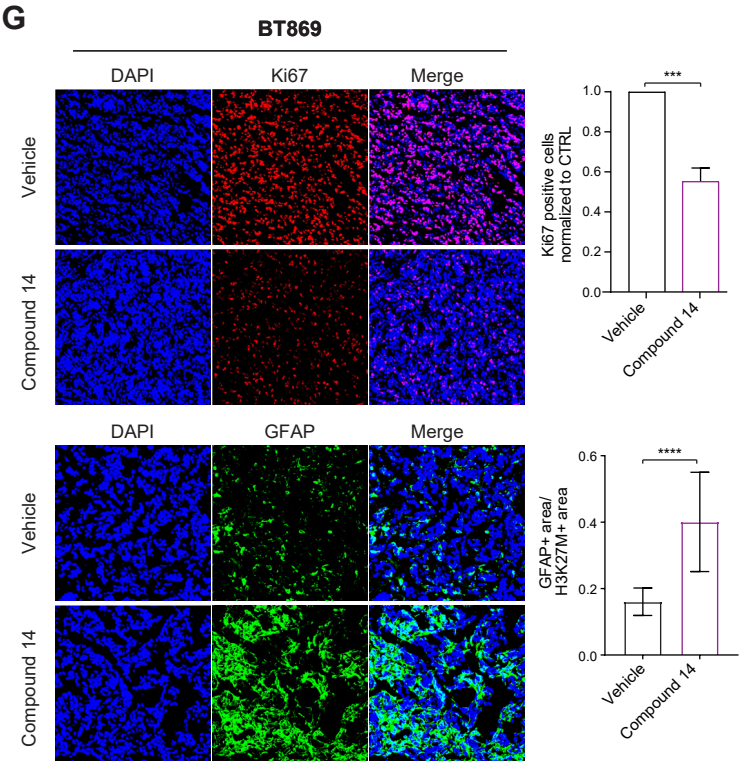

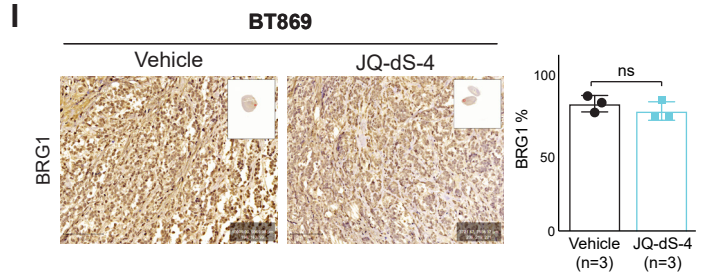

J

Kinetic solubility studies

Compound	Media	Visual Appearance	Kinetic Solubility (μM)
Compound 11	PBS (pH 7.4)	no visible particles	177
Compound 14	PBS (pH 7.4)	many visible particles	97.3
JQ-dS-4	PBS (pH 7.4)	many visible particles	<1.56

Supplementary figure 6. A. Mass spectrometry multiple reaction monitoring imaging was used to assess the penetration of Compound 11 in non-tumor bearing mouse brain tissue. Calibration curve of Compound 11 from the spiked tissue homogenate mimetic is shown in the top panel. H&E staining and MALDI MSI ion images of heme b and Compound 11 from coronal sections are shown in the bottom panel. An average of 1.3 ± 0.2 μM (n = 2) of Compound 11 was detected in the dosed animals, which is lower than the established limit of quantification. Heme b distribution was mapped for each sample to visualize the brain vasculature for the assessment of drug penetration. **B.** Percentage of drug present in the brain (compared to plasma) in non-tumor bearing mice dosed intraperitoneally with 5 mg/kg of indicated chemical compounds for 2 hours as assessed by mass spectrometry multiple reaction monitoring imaging. **C.** H&E and Ki67 immunostaining of BT869 subcutaneous xenograft model. **D.** Body weight measurements in BT869 subcutaneous tumor bearing mice treated with either vehicle control, Compound 14 (20 mg/kg IP daily) or JQ-dS-4 (50 mg/kg IP daily) for 45 days (n=10 per group). Data are shown as mean +/- SEM. **E.** Tumor volume measured after 45 days of Compound 14 treatment (20 mg/kg IP daily), compared to vehicle control in mice bearing HSJD-DIPG007 (H3.3K27M) subcutaneous tumors. p-value = 0.0146 (unpaired t-test). **F.** Representative immunostaining (left panels) and corresponding quantification (right panel) of cleaved caspase 3 in BT869 subcutaneous mice treated for 10-days (pharmacodynamic assessment cohort, n=3 per group) with Compound 14 (20 mg/kg IP daily), compared to vehicle controls. **G**. Representative immunostaining for nuclei (DAPI) and proliferation marker (Ki67) or AC-like marker (GFAP) in treated mice bearing BT869 subcutaneous tumors. Mice were treated with Compound 14 (20 mg/kg IP daily) or vehicle for 10 days and collected for pharmacodynamic assessment. Three mice were analyzed per group; four sections were analyzed to obtain 10,000 cells per tumor, resulting in 12 measurements per group. Quantification of immunofluorescence signal are shown as mean +/- SD; p-value of 0.0003 for Ki67 and < 0.0001 for GFAP (unpaired t-test). **H.** Representative immunostaining for nuclei (DAPI) and proliferation marker (Ki67) or AC-like marker (GFAP) in treated mice bearing HSJD-DIPG007 subcutaneous tumors. Mice were treated with Compound 14 (20 mg/kg IP daily) or vehicle and collected at end stage disease. Two mice were analyzed per group; two sections were analyzed per tumor to obtain 10,000 cells per tumor, resulting in 4 measurements per group. Quantification of immunofluorescence signal are shown as mean +/- SD; p-value of 0.0014 for Ki67 and 0.0033 for GFAP (unpaired t-test). **I.** Representative immunostaining

(left panels) and corresponding quantification (right panel) of BRG1 in JQ-dS-4 (50 mg/kg IP daily) treated BT869 subcutaneous tumors compared to vehicle controls. **J**. Results from kinetic solubility studies performed with Compound 11, Compound 14, and JQ-dS-4.